

Fundamental constants and tests of theory in Rydberg states of hydrogen-like ions

Ulrich D. Jentschura,^{1,2} Peter J. Mohr,¹ Joseph N. Tan,¹ and Benedikt J. Wundt²

¹National Institute of Standards and Technology, Gaithersburg, MD 20899-8420, USA

²Max-Planck-Institut für Kernphysik, Saupfercheckweg 1, 69117 Heidelberg, Germany

(Dated: February 12, 2022)

Comparison of precision frequency measurements to quantum electrodynamics (QED) predictions for Rydberg states of hydrogen-like ions can yield information on values of fundamental constants and test theory. With the results of a calculation of a key QED contribution reported here, the uncertainty in the theory of the energy levels is reduced to a level where such a comparison can yield an improved value of the Rydberg constant.

PACS numbers: 12.20.Ds, 31.30.Jv, 06.20.Jr, 31.15.-p

Quantum electrodynamics (QED) makes extremely accurate predictions despite the “mathematical inconsistencies and renormalized infinities swept under the rug” [1]. With the assumption that the theory is correct, it is used to determine values of the relevant fundamental constants by adjusting their values to give the best agreement with experiments [2]. In this paper, we consider the possibility of making such comparisons of theory and experiment for Rydberg states of cooled hydrogen-like ions using an optical frequency comb. We find that because of simplifications in the theory that occur for Rydberg states, together with the results of a calculation reported here, the uncertainty in the predictions of the energy levels is dominated by the uncertainty in the Rydberg constant, the electron-nucleus mass ratio, and the fine-structure constant. Apart from these sources of uncertainty, to the extent that the theory remains valid, the predictions for the energy levels appear to have uncertainties as small as parts in 10^{17} in the most favorable cases.

The CODATA recommended value of the Rydberg constant has been obtained primarily by comparing theory and experiment for twenty-three transition frequencies or pairs of frequencies in hydrogen and deuterium [2]. The theoretical value for each transition is the product of the Rydberg constant and a calculated factor based on QED that also depends on other constants. While the most accurately measured transition frequency in hydrogen (1S–2S) has a relative uncertainty of 1.4×10^{-14} [3], the recommended value of the Rydberg constant has a larger relative uncertainty of 6.6×10^{-12} which is essentially the uncertainty in the theoretical factor. The main source is the uncertainty in the charge radius of the proton with additional uncertainty due to uncalculated or partially calculated higher-order terms in the QED corrections. This uncertainty could be reduced by a measurement of the proton radius in muonic hydrogen [4], or by a sufficiently accurate measurement of a different transition in hydrogen. On the other hand, for Rydberg states, the fact that the wave function is small near the nucleus results in the finite nuclear size correction being completely negligible. Also, for Rydberg states, the higher-order terms in the QED corrections are relatively smaller than they are for S states, so theoretical expressions with a given number of terms are more accurate.

Circular Rydberg states of hydrogen in an 80 K atomic beam have been studied with high precision for transition

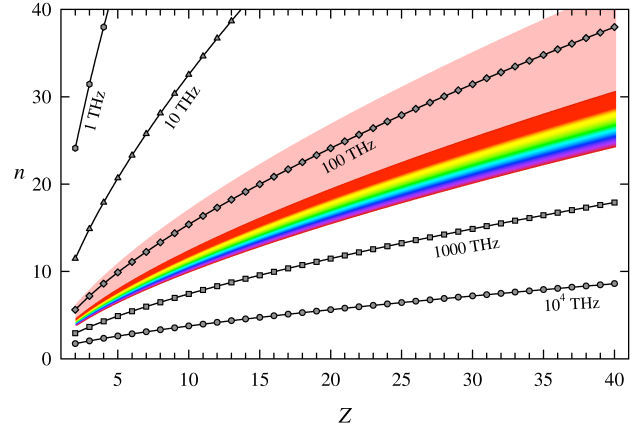


FIG. 1: Graph showing values of Z and approximate n that give a specified value of the frequency for transitions between states with principal quantum number n and $n - 1$ in a hydrogen-like ion with nuclear charge Z . Frequencies in the near infrared and visible range are indicated in color.

wavelengths in the millimeter region, providing a determination of the Rydberg constant with a relative uncertainty of 2.1×10^{-11} [5, 6]. With the advent of optical frequency combs [7], precision measurements of optical transitions between Rydberg states have now become possible using femtosecond lasers. An illustration is the laser spectroscopy of antiprotonic helium [8]. Figure 1 gives iso-frequency curves corresponding to the spacing between adjacent Bohr energy levels (n to $n - 1$) in the 2-dimensional parameter space of the principal quantum number n and the nuclear charge Z for hydrogen-like ions. Much of this space is accessible to optical frequency synthesizers based on mode-locked femtosecond lasers, which readily provide ultra-precise reference rulers spanning the near-infrared and visible region of the optical spectrum (530 nm–2100 nm). Diverse techniques in spectroscopy (such as double-resonance methods) broaden the range of applications. Even when the absolute accuracy is limited by the primary frequency standard (a few parts in 10^{16}), optical frequency combs can enable relative frequency measurements with uncertainties approaching 1 part in 10^{19} over 100 THz of bandwidth [9]. The precisely controlled pulse train from a femtosecond laser can also be used directly to

probe the global atomic structure, thus integrating the optical, terahertz, and radio-frequency domains [10].

There are simplifications in the theory of energy levels of Rydberg states of hydrogen-like ions that, in some cases, allow calculations to be made at levels of accuracy comparable to these breakthroughs in optical metrology. In the following, we write the known theoretical expressions for the energy levels of these ions, describe and give results of a calculation that eliminates the largest source of uncertainty, and list the largest remaining sources of uncertainty. We also make numerical predictions for a transition in two different ions as illustrations, look at the natural line width, and discuss what might be learned from comparison of theory and experiment.

In a high- n Rydberg state of a hydrogen-like atom with nuclear charge Z and angular momentum $l = n - 1$, the probability of the electron being within a short distance r from the origin is of order $(2Zr/na_0)^{2n+1}/(2n+1)!$, where a_0 is the Bohr radius. Due to this strong damping near the origin, effects arising from interactions near or inside the nucleus are negligible, including the effect of the finite size of the nucleus.

For $l \geq 2$, the theoretical energy levels can be accurately expressed as a sum of the Dirac energy with nuclear motion corrections E_{DM} , relativistic recoil corrections E_{RR} , and radiative corrections E_{QED} : $E_n = E_{\text{DM}} + E_{\text{RR}} + E_{\text{QED}}$. Reviews of the theory and references to original work are given in [2, 11, 12]. The difference between the Dirac eigenvalue and the electron rest energy is proportional to

$$\alpha^2 D = \left[1 + \frac{(Z\alpha)^2}{(n-\delta)^2} \right]^{-\frac{1}{2}} - 1 \quad (1)$$

$$D = -\frac{Z^2}{2n^2} + \left(\frac{3}{8n} - \frac{1}{2j+1} \right) \frac{Z^4 \alpha^2}{n^3} + \dots,$$

where α is the fine-structure constant, $\delta = |\kappa| - \sqrt{\kappa^2 - (Z\alpha)^2}$, $\kappa = (-1)^{l+j+1/2}(j+1/2)$ is the Dirac spin-angular quantum number, and j is the total angular momentum quantum number. The energy level, taking into account the leading nuclear motion effects, but not including the electron or nucleus rest energy, is given by [12]

$$E_{\text{DM}} = 2hcR_\infty \left[\mu_r D - \frac{r_N \mu_r^3 \alpha^2}{2} D^2 + \frac{r_N^2 \mu_r^3 Z^4 \alpha^2}{2n^3 \kappa (2l+1)} \right], \quad (2)$$

where h is the Planck constant, c is the speed of light, $R_\infty = \alpha^2 m_e c / 2h$ is the Rydberg constant, $r_N = m_e / m_N$ is the ratio of the electron mass to the nucleus mass, and $\mu_r = 1/(1+r_N)$ is the ratio of the reduced mass to the electron mass.

Relativistic corrections to Eq. (2) associated with motion of the nucleus are classified as relativistic-recoil corrections. For the states with $l \geq 2$ under consideration here, we have

$$E_{\text{RR}} = 2hcR_\infty \frac{r_N Z^5 \alpha^3}{\pi n^3} \left\{ \mu_r^3 \left[-\frac{8}{3} \ln k_0(n, l) - \frac{7}{3l(l+1)(2l+1)} \right] \right\} \quad (3)$$

$$+ \pi Z\alpha \left[3 - \frac{l(l+1)}{n^2} \right] \frac{2}{(4l^2-1)(2l+3)} + \dots \Bigg\},$$

where $\ln k_0(n, l)$ is the Bethe logarithm. We assume that the uncertainty due to uncalculated higher-order terms is $Z\alpha \ln(Z\alpha)^{-2}$ times the contribution of the last term in Eq. (3).

Quantum electrodynamics (QED) corrections for high- l states are summarized as

$$E_{\text{QED}} = 2hcR_\infty \frac{Z^4 \alpha^2}{n^3} \left\{ -\mu_r^2 \frac{a_e}{\kappa(2l+1)} + \mu_r^3 \frac{\alpha}{\pi} \left[-\frac{4}{3} \ln k_0(n, l) + \frac{32}{3} \frac{3n^2 - l(l+1)}{n^2} \times \frac{(2l-2)!}{(2l+3)!} (Z\alpha)^2 \ln \left[\frac{1}{\mu_r (Z\alpha)^2} \right] + (Z\alpha)^2 G(Z\alpha) \right] \right\}, \quad (4)$$

where a_e is the electron magnetic moment anomaly and $G(Z\alpha)$ is a function that contains higher-order QED corrections. Equation (4) contains no explicit vacuum polarization contribution because of the damping of the wavefunction near the origin. Also in that equation, the uncertainties in the theory of a_e may be eliminated by using the experimental value $a_e = 1.159\,652\,180\,85(76) \times 10^{-3}$ obtained with a one-electron quantum cyclotron [13].

The leading terms in $G(Z\alpha)$ are expected to be of the form

$$G(Z\alpha) = A_{60} + A_{81}(Z\alpha)^2 \ln(Z\alpha)^{-2} + A_{80}(Z\alpha)^2 + \dots + \frac{\alpha}{\pi} B_{60} + \dots + \left(\frac{\alpha}{\pi} \right)^2 C_{60} + \dots \quad (5)$$

The coefficients indicated by the letter A arise from the one-photon QED corrections; A_{60} and A_{81} arise from the self energy, and A_{80} arises from both the self energy and the long-range component of the vacuum polarization. The term A_{60} has been calculated for many states with $l \leq 8$, but not for higher- l states before this work. The uncertainty introduced by this term if it were not calculated, based on plausible extrapolations from lower- l known values, would be the largest uncertainty in the theory and larger than the uncertainty from the Rydberg constant. The higher-order coefficient A_{81} and the self-energy component of the coefficient A_{80} are not known, but can be expected to be small. The vacuum polarization contribution to A_{80} is known [14] and is extremely small. The coefficient B_{60} arises from two-photon diagrams and has not been calculated for high- l states, but a comparison of calculated values of B_{60} [15] and A_{60} [16] for $l \leq 5$, suggests it has a magnitude of roughly $4A_{60}$, which is used as the associated uncertainty. Further, a term proportional to $(\alpha/\pi)B_{61} \ln(Z\alpha)^{-2}$, that is nonzero for S and P states, vanishes for higher- l states [17]. The term C_{60} is expected to be the next three-photon term, in analogy with the two-photon terms.

In order to eliminate the main source of theoretical uncertainty in the energy levels, we have calculated the value of A_{60} for a number of Rydberg states. This calculation uses

TABLE I: Calculated values of the constant A_{60} . The numbers in parentheses are standard uncertainties in the last figure.

n	l	$2j$	κ	A_{60}	$2j$	κ	A_{60}
13	11	21	11	$0.679\,575(5) \times 10^{-5}$	23	-12	$4.318\,998(5) \times 10^{-5}$
13	12	23	12	$0.469\,973(5) \times 10^{-5}$	25	-13	$2.729\,475(5) \times 10^{-5}$
14	12	23	12	$0.410\,825(5) \times 10^{-5}$	25	-13	$2.979\,937(5) \times 10^{-5}$
14	13	25	13	$0.296\,641(5) \times 10^{-5}$	27	-14	$1.945\,279(5) \times 10^{-5}$
15	13	25	13	$0.252\,108(5) \times 10^{-5}$	27	-14	$2.116\,050(5) \times 10^{-5}$
15	14	27	14	$0.189\,309(5) \times 10^{-5}$	29	-15	$1.420\,631(5) \times 10^{-5}$
16	14	27	14	$0.155\,786(5) \times 10^{-5}$	29	-15	$1.540\,181(5) \times 10^{-5}$
16	15	29	15	$0.121\,749(5) \times 10^{-5}$	31	-16	$1.059\,674(5) \times 10^{-5}$

methods from field theory, *i.e.*, nonrelativistic QED (NRQED) effective operators which facilitate the calculation [18], and methods from atomic physics to handle the extensive angular momentum algebra in the higher-order binding corrections of near-circular Rydberg states. Distinct contributions to the self-energy from high- and low-energy virtual photons, are matched using an intermediate cutoff parameter [19]. For near-circular Rydberg states, the radial wave functions have at most a few nodes, yet the calculation of A_{60} coefficients for these states is much more involved than for low-lying states. The reason is that in using the Sturmian decomposition of the hydrogen Coulomb Green function, as done for lower- n states, the radial integrations lead to sums over hypergeometric functions with high indices, which in turn give rise to an excessive number of terms. For states with $n = 8$, there are of order 10^5 terms in intermediate steps, which is roughly two orders of magnitude more terms than for states with $n = 2$ [20]. This trend continues as n increases making calculation at high n with this conventional method intractable.

Here we report that the calculation has been done with a combined analytic and numerical approach based on lattice methods by using a formulation of the Schrödinger-Coulomb Green function on a numerical grid [21]. Provided quadruple precision (~ 32 significant digits) in the Fortran code is used, and provided a large enough box to represent the Rydberg states on the grid is used, the positive continuum of states can be accurately represented by a pseudo-spectrum of states with positive discrete energies. With this basis set, the virtual photon energy integration can be carried out analytically for each pseudo-state using Cauchy's theorem. This solves the problem of the calculation of the relativistic Bethe logarithms without the need for the subtraction of many pole terms, which would otherwise be necessary if the virtual photon energy were used as an explicit numerical integration variable. The results of this calculation for a number of states with $n = 13$ to 16 are given in Table I.

We incorporate the results for A_{60} to numerically evaluate the theoretical prediction for the frequency of the transition between the state with $n = 14$, $l = 13$, $j = \frac{27}{2}$ and the state with $n = 15$, $l = 14$, $j = \frac{29}{2}$ in the hydrogen-like ions He^+ and Ne^{9+} . The constants used in the evaluation are the 2006 CODATA recommended values [22], with the exception of the neon nucleus mass $m(^{20}\text{Ne}^{10+})$ which is taken from the

TABLE II: Transition frequencies between the highest- j states with $n = 14$ and $n = 15$ in hydrogen-like helium and hydrogen-like neon.

Term	$^4\text{He}^+ \nu(\text{THz})$	$^{20}\text{Ne}^{9+} \nu(\text{THz})$
E_{DM}	8.652 370 766 008(58)	216.335 625 5746(14)
E_{RR}	0.000 000 000 000	0.000 000 000 1
E_{QED}	-0.000 000 001 894	-0.000 001 184 1
Total	8.652 370 764 114(58)	216.335 624 3907(14)

neon atomic mass [23], corrected for the mass of the electrons and their binding energies. Values of the various contributions and the total are given as frequencies in Table II. Standard uncertainties are listed with the numbers where they are non-negligible. The theory is sufficiently accurate that the largest uncertainty arises from the Rydberg frequency cR_∞ , which is a factor in all of the contributions. There is no uncertainty from the Planck constant, since $\nu = (E_{15} - E_{14})/h$.

Table III gives sources and estimates of the various known uncertainties in the theory. To put them in perspective, in hydrogen, the relative uncertainty from the two-photon term B_{60} for the 1S–2S transition is of the order of 10^{-12} due to disagreement between different calculations, whereas in the $n = 14$ to $n = 15$ Rydberg transition it is likely to be roughly 5×10^{-19} , based on the smallness of the calculated value of the A_{60} coefficient. The improved convergence of the expansion of the QED corrections in powers of $Z\alpha$ is indicated by the fact that A_{60} is smaller by a factor of about 10^6 for the Rydberg states than the value $A_{60} \approx -30$ for S states.

The QED level shift given by Eq. (4) is understood to be the real part of the radiative correction, while the complete radiative correction to the level $\mathcal{E}_{\text{QED}} = E_{\text{QED}} - i\Gamma/2$ is complex and includes an imaginary part proportional to the rate $A = \Gamma/\hbar$ for spontaneous radiative decay of the level to all lower levels. For the highest- l state with principal quantum number n , the dominant decay mode is an E1 decay to the highest- l state with principal quantum number $n-1$ [24]. Formulas in Ref. [24] give the nonrelativistic expression for the decay rate, which can also be derived from the nonrelativistic limit of the imaginary part of the level shift [25].

As a first approximation, for transitions between states with quantum numbers n and $n-1$ the ratio of the transition energy

TABLE III: Sources and estimated relative standard uncertainties in the theoretical value of the transition frequency between the highest- j states with $n = 14$ and $n = 15$ in hydrogen-like helium and hydrogen-like neon.

Source	He^+	Ne^{9+}
Rydberg constant	6.6×10^{-12}	6.6×10^{-12}
Fine-structure constant	7.0×10^{-16}	1.7×10^{-14}
Electron-nucleus mass ratio	5.8×10^{-14}	1.2×10^{-14}
a_e	1.4×10^{-19}	3.5×10^{-18}
Theory: E_{RR} higher order	6.2×10^{-17}	2.4×10^{-14}
Theory: $E_{\text{QED}} A_{81}$	1.7×10^{-18}	1.6×10^{-14}
Theory: $E_{\text{QED}} B_{60}$	8.6×10^{-18}	5.4×10^{-15}

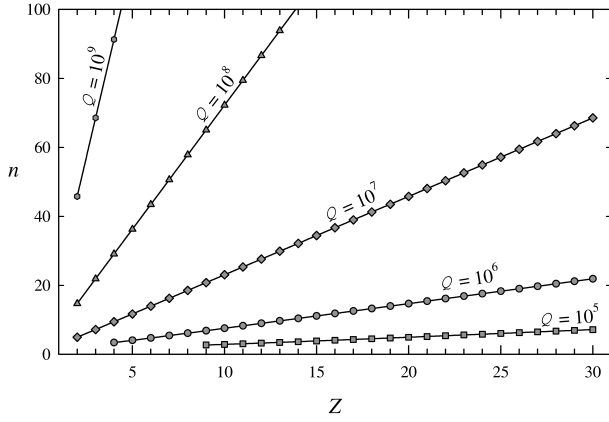


FIG. 2: Graph showing values of Z and approximate n that give a specified ratio of the transition frequency to the natural width of the transition resonance between circular states with principal quantum number n and $n - 1$ in a hydrogen-like ion with nuclear charge Z .

to the width of the line, is given by

$$Q = \frac{E_n - E_{n-1}}{\Gamma_n + \Gamma_{n-1}} \rightarrow \frac{3n^2}{4\alpha(Z\alpha)^2} + \dots, \quad (6)$$

where the expression on the right is the asymptotic form as $n \rightarrow \infty$ of the nonrelativistic value. Figure 2 gives a contour plot of the values of n and Z that give a specified value of Q based on the nonrelativistic result in Ref. [24]. This is just a rough indication, since transitions with smaller l values will generally have a smaller Q , whereas transitions with a change of n greater than 1 will have a larger Q . The effect of possible asymmetries of the line shape on the apparent resonance center has been shown to be small by Low [26], of order $\alpha(Z\alpha)^2 E_{\text{QED}}$. For the 1S–2S transition in hydrogen, such effects are indeed completely negligible at the current level of experimental accuracy [27]. However, for Rydberg states of hydrogen-like ions, particularly at higher- Z , asymmetries in the line shape, some of which depend on details of the experiment, may be significant, and can be calculated if necessary.

Recent advances in atomic-molecular-optical physics have generated an array of tools and techniques useful for engineering highly simplified atomic systems [28]. In particular, observations of cold antihydrogen production at CERN illustrate two ways for a cooled ion/antiproton to capture an electron/positron in high- l Rydberg states, either by three-body recombination or by charge exchange [29]. Properties of atomic cores have also been studied using a double-resonance detection technique to observe the fine structure of Rydberg states produced by charge exchange in a fast beam of highly-charged ions [30]. Using electron cooling [29] (and charge exchange), cold hydrogen-like ions can be recombined in high- l Rydberg states from a variety of bare ions extracted from sources such as an electron beam ion source/trap (EBIS/T). Although two-photon spectroscopy is possible in certain cases, if the ions are confined in a trap within a region smaller than about half

the wavelength of the radiation exciting the transition, Dicke narrowing also eliminates the first-order Doppler shift [31]. Assuming $T = 100$ K, the relative second-order Doppler shift is about 3.5×10^{-12} for He^+ and 7×10^{-13} for Ne^{9+} . Temperatures in the range $4 \text{ K} < T < 77 \text{ K}$ are obtainable in cryogenic ion traps by resistive cooling [31] and by electron or positron cooling [29]. For lower temperatures ($T < 1 \text{ K}$), sympathetic laser cooling methods can be used [31].

Of the variety of (n, l, Z) combinations of hydrogen-like ions, circular Rydberg states of low- Z ions seem the most favorable for a comb-based determination of the Rydberg constant. On the other hand, some perturbations are smaller and line-widths are larger in heavier ions. Hence, using ions with a variety of (n, Z) combinations could be useful for experimental optimization and consistency checks, as well as for extending diversity of experiments used to determine fundamental constants and test theory.

UDJ acknowledges support from the Deutsche Forschungsgemeinschaft (Heisenberg program). Mr. Frank Bellamy provided assistance with some of the numerical evaluations.

-
- [1] F. Dyson, letter to G. Gabrielse, July 15 (2006).
 - [2] P. J. Mohr and B. N. Taylor, *Rev. Mod. Phys.* **77**, 1 (2005).
 - [3] T. Hänsch *et al.*, *Philos. Trans. R. Soc. London, Ser. A* **363**, 2155 (2005).
 - [4] T. Nebel *et al.*, *Can. J. Phys.* **85**, 469 (2007).
 - [5] D. Kleppner, private communication (2003).
 - [6] J. C. De Vries, Ph.D. thesis, MIT (2001).
 - [7] T. W. Hänsch, *Rev. Mod. Phys.* **78**, 1297 (2006).
 - [8] M. Hori *et al.*, *Phys. Rev. Lett.* **96**, 243401 (2006).
 - [9] L.-S. Ma *et al.*, *Science* **303**, 1843 (2004).
 - [10] A. Marian *et al.*, *Science* **306**, 2063 (2004).
 - [11] J. R. Sapirstein and D. R. Yennie, in *Quantum Electrodynamics*, edited by T. Kinoshita (World Scientific, Singapore, 1990), chap. 12, pp. 560–672.
 - [12] M. I. Eides *et al.*, *Phys. Rep.* **342**, 63 (2001).
 - [13] B. Odom *et al.*, *Phys. Rev. Lett.* **97**, 030801 (2006).
 - [14] E. H. Wichmann and N. M. Kroll, *Phys. Rev.* **101**, 843 (1956).
 - [15] U. D. Jentschura, *Phys. Rev. A* **74**, 062517 (2006).
 - [16] E.-O. Le Bigot *et al.*, *Phys. Rev. A* **68**, 042101 (2003).
 - [17] U. D. Jentschura *et al.*, *Phys. Rev. A* **72**, 062102 (2005).
 - [18] W. Caswell and G. Lepage, *Phys. Lett. B* **167B**, 437 (1986).
 - [19] B. J. Wundt and U. D. Jentschura, arXiv:0710.1864 (2007).
 - [20] U. D. Jentschura *et al.*, *Phys. Rev. Lett.* **90**, 163001 (2003).
 - [21] S. Salomonson and P. Öster, *Phys. Rev. A* **40**, 5559 (1989).
 - [22] <http://physics.nist.gov/constants>.
 - [23] G. Audi *et al.*, *Nucl. Phys. A* **729**, 337 (2003).
 - [24] H. A. Bethe and E. E. Salpeter, *Quantum Mechanics of One- and Two-electron Atoms* (Academic Press, New York, 1957).
 - [25] U. D. Jentschura *et al.*, *J. Phys. B* **38**, S97 (2005).
 - [26] F. Low, *Phys. Rev.* **88**, 53 (1952).
 - [27] U. D. Jentschura and P. J. Mohr, *Can. J. Phys.* **80**, 633 (2002).
 - [28] AMO2010, *Controlling the Quantum World* (National Academies Press, Washington, DC, 2007).
 - [29] G. Gabrielse, *Adv. At. Mol. Opt. Phys.*, **50**, 155 (2005).
 - [30] S. R. Lundeen and C. W. Fehrenbach, *Phys. Rev. A* **75**, 032523 (2007).
 - [31] W. M. Itano, *et al.*, *Phys. Scripta* **T59**, 106 (1995).